VERSITA

Biologia **68**/6: 1104—1108, 2013
Section Botany
DOI: 10.2478/s11756-013-0254-7

Pines influence hydrophysical parameters and water flow in a sandy soil**

Ľubomír Lichner[1]*, Jozef Capuliak[2], Natalia Zhukova[3], Ladislav Holko[1], Henryk Czachor[4] & Jozef Kollár[5]

[1]*Institute of Hydrology, Slovak Academy of Sciences, Račianska 75, SK-83102 Bratislava, Slovakia; e-mail: lichner@uh.savba.sk*
[2]*National Forestry Centre, T.G. Masaryka 22, SK-96092 Zvolen, Slovakia*
[3]*M. Nodia Institute of Geophysics, 1 Alexidze str., 0193 Tbilisi, Georgia*
[4]*Institute of Agrophysics, Polish Academy of Sciences, Doswiadczalna 4, PL-20236 Lublin, Poland*
[5]*Institute of Landscape Ecology, Slovak Academy of Sciences, Štefánikova 3, SK-81499 Bratislava, Slovakia*

Abstract: Pines, used for sand dune stabilization, can influence the hydrophysical parameters and water flow in an aeolian sandy soil considerably, mainly due to soil water repellency. Two sites, separated by distance of about 20 m, formed the basis of our study. A control soil ("Pure sand") with limited impact of vegetation or organic matter was formed at 50 cm depth beneath a forest glade area. This was compared to a "Forest soil" in a 30-year old Scots pine (*Pinus sylvestris*) forest. Most of the hydrophysical parameters were substantially different between the two soil surfaces. The forest soil was substantially more water repellent and had two-times the degree of preferential flow compared to pure sand. Water and ethanol sorptivities, hydraulic conductivity, and saturated hydraulic conductivity were 1%, 84%, 2% and 26% those of the pure sand, respectively. The change in soil hydrophysical parameters due to soil water repellency resulted in preferential flow in the forest soil, emerging during a simulated heavy rain following a long hot, dry period. The wetting front established in pure sand exhibited a form typical of that for stable flow. Such a shape of the wetting front can be expected in the forest soil in spring, when soil water repellency is alleviated substantially.

Key words: hydrophysical parameters; pine; preferential flow; sandy soil; water repellency

Introduction

Pines are widely planted for sand dune stabilization (CAB International 2002). Previous studies in sandy soil beneath Scots pine (*Pinus sylvestris*) trees showed that both soil water repellency and hydraulic properties depend on tree age, forest management practices, and the season of the year (Buczko et al. 2006). Soil water repellency can decrease infiltration, increase runoff and soil erosion, and worsen water quality (Doerr et al. 2000; Pekárová et al. 2012; Wine et al. 2012; Beatty & Smith 2013). Remediation strategies for soil water repellency were reviewed by Müller & Deurer (2011). The objective of this study was to quantify the influence of Scots pines on soil hydrophysical parameters and heterogeneity of water flow in a sandy soil emerging during a simulated heavy rain following a long hot, dry period.

Material and methods

The experimental sites were located at Mláky II near Sekule (48°37′10″ N, 16°59′50″ E) in the Borská nížina lowland (southwest Slovakia). The region is in transition zone between temperate oceanic and continental climates. Mean annual temperature is 9 °C. Mean annual precipitation is 550 mm, and it is mainly summer-dominant. Two sites, separated by distance of about 20 m, formed the basis of our study. A control soil ("Pure sand") with limited impact of vegetation or organic matter was obtained by sampling at 50 cm depth beneath a forest glade area. This was compared to a "Forest soil" in a 30-year old Scots pine (*Pinus sylvestris*) forest. The soil at the glade area supported a sparse cover of mosses, lichens, and occasionally, grasses (*Corynephorus canescens*). Some areas in the glade had exposed bare soil. Soil microscopic mosses, lichens, fungi, cyanobacteria, and algae, recorded at this site, are listed in Lichner et al. (2012). Soil from the experimental sites is formed by aeolian sand, and it is classified as an Arenosol (WRB 2006) and has a sandy texture (Soil Survey Division Staff 1993). Physical and chemical properties of soil samples are presented in Table 1.

The persistence of water repellency was measured using the water drop penetration time (WDPT) test. The WDPT test involves placing a water drop from a standard medicine dropper on a soil surface and recording the time taken for its complete penetration (Doerr et al. 2000). The following classes of the persistence of WR can be distinguished: wettable or non-water-repellent soil (WDPT $<$ 5 s); slightly

*Corresponding author, **Special Section on Biohydrology, guest-editors Ľubomír Lichner & Kálmán Rajkai

Table 1. Physical and chemical properties of soil from the studied sites.

Site	Depth (cm)	Sand (%)	Silt (%)	Clay (%)	$CaCO_3$ (%)	C (%)	pH (H_2O)	pH (KCl)
Forest soil	0–1	95.14	2.26	2.60	<0.05	0.83	5.65	4.39
Pure sand	50–55	94.86	1.74	3.40	<0.05	0.03	5.54	4.20

(WDPT = 5–60 s), strongly (WDPT = 60–600 s), severely (WDPT = 600–3600 s), and extremely (WDPT > 3600 s) water repellent soil (García et al. 2005).

Field measurements of infiltration were performed using a minidisk infiltrometer (4.5 cm in diameter) under a negative tension $h_0 = -2$ cm. Prior to the measurements, the litter layer was removed gently to prevent disturbance of the mineral soil. The cumulative infiltration I was calculated based on the Philip infiltration equation:

$$I = C_1 t^{1/2} + C_2 t + C_3 t^{3/2} + \cdots + C_m t^{m/2} + \cdots \quad (1)$$

where C_1, C_2, C_3,..., and C_m are coefficients, and t is time.

The sorptivity $S(h_0)$ was estimated from the first term of this equation ($I = C_1 t^{1/2}$):

$$S(h_0) = I/t^{1/2} \quad (2)$$

Equation (2) was used to calculate the sorptivity of both water, $S_w(-2\text{ cm})$, and ethanol, $S_e(-2\text{ cm})$, from the cumulative infiltration *vs.* time relationships taken with the minidisk infiltrometer during early-time (< 180 s) infiltration of water and ethanol, respectively.

Zhang (1997) proposed to use first two terms of the Philip infiltration equation to fit the cumulative infiltration *vs.* time relationship and estimate the hydraulic conductivity $k(h_0)$:

$$k(h_0) = C_2/A \quad (3)$$

where A is a dimensionless coefficient. Equation (3) was used to estimate the hydraulic conductivity $k(-2\text{ cm})$ in this study, using $A = 1.8$ for sandy soil and suction $h_0 = -2$ cm from the Minidisk Infiltrometer User's Manual (Decagon 2007).

The index of water repellency R was calculated from (Hallett et al. 2001):

$$R = 1.95 S_e(-2\text{ cm})/S_w(-2\text{ cm}) \quad (4)$$

Infiltration measurements in the field under a small positive pressure head $h_0 = +2$ cm were also performed repeatedly at both sites using a double-ring infiltrometer with an inner-ring diameter of 24.5 cm, buffer ring diameter of 34.5 cm, and height of 23.5 cm. The first two and three terms of the Philip infiltration equation were used to estimate the saturated hydraulic conductivity K_s. The first two terms are applicable to relatively short times as follows:

$$I \approx S t^{1/2} + m K_s t \quad (5)$$

with $m = 0.667$ being the most frequently used value (Kutílek & Nielsen 1994).

Kutílek & Krejča (1987) proposed to use three terms of the Philip infiltration equation to estimate the saturated hydraulic conductivity K_s:

$$K_s \approx (3C_1C_3)^{1/2} + C_2 \quad (6)$$

Equations (5) and (6) were used to estimate the saturated hydraulic conductivity K_s in this study.

The tracer experiment at the forest site was carried out at the 100 cm × 100 cm plot and it is described in Homolák et al. (2009). The tracer experiment in pure sand was carried out at the 50 cm × 100 cm plot and it is described in Lichner et al. (2011). The effective cross section for water flow, ECS, and the degree of preferential flow, DPF, were determined from the stained area as follows. The picture of each vertical section was divided to $i = 10$ vertical bands with the width of 10 cm, and the numbers n_i of stained 5 cm × 5 cm pixels were calculated in each band. The fraction of total water content change f_i, which is the ratio between the water content change in band i and the total water content change in vertical profile, was calculated for each band using

$$f_i = n_i / \sum_{i=1}^{i=10} n_i \quad \text{with} \quad \sum_{i=1}^{i=10} f_i = 1 \quad (7)$$

The fractions f_i were ranked in descending order and presented against the fraction of cross-sectional area (black dots at Fig. 1b). A beta distribution was fitted to the data and the Levenberg-Marquardt algorithm (the non-linear least-square fitting) was used to optimize its parameters α and β. ECS was then estimated as the fraction of the total area that corresponds to the 90% of water content change in vertical section (*cf.* Fig. 1b), according to the definition in Täumer et al. (2006).

The degree of preferential flow, DPF, equal to the area between the beta distribution curve and the 1:1 line (representing the distribution of fraction of total water content change *vs.* fraction of cross-sectional area for a piston flow), was calculated from (*cf.* Fig. 1b)

$$\text{DPF} = \int_{x=0}^{1} p(x;\alpha,\beta)\mathrm{d}x - 0.5 \quad (8)$$

DPF can change from 0 for piston flow to almost 0.5 for the case when all the flow in soil is realized through a narrow preferential path (e.g., a crack in heavy clay soil).

A Student t-test (Matlab) was used to determine whether the results differed significantly between the two sites. Levene's test (Levene 1960) and Q-Q plot were used to test whether the data were normally distributed with homogenous variances. The data that did not pass the test were transformed using the Box-Cox method based on estimation and minimization of standard deviation of the function under underlying transformation. Then, the t-test was used to compare the means and variances of the above data from the two sites to find out whether they were statistically significantly different.

Results and discussion

The hydrological properties of the soil at both sites are presented in Table 2, where N is a number of replicates.

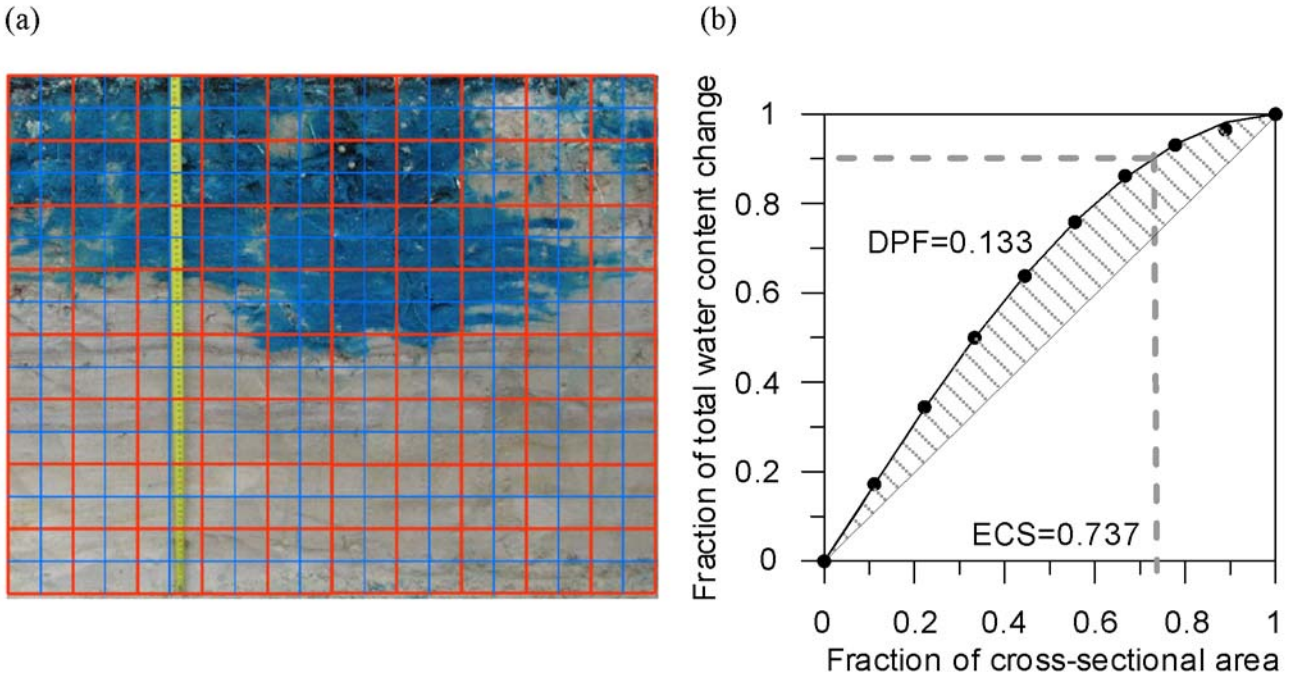

Fig. 1. Estimation of effective cross section (ECS) and degree of preferential flow (DPF) from the image of a vertical section of dyed soil, taken in the forest soil at the distance of 60 cm from the front edge during the tracer experiment. a) – the image of the vertical section with 10 cm (red lines) and 5 cm (blue lines) grids used for an estimation of the fractions of total water content change against the fractions of total cross-sectional area; b) – the plot of the cumulative water content changes against the cumulative cross-sectional area (black dots), with ECS estimated as the fraction of the total cross-sectional area that corresponds to the 90% of total water content change, and DPF presented as the shaded area between beta-function fitted to the data and straight line representing the piston flow.

Table 2. Statistical parameters of hydrophysical properties for the two studied sites.

Site	Attribute	Minimum value	Maximum value	Median	Arithmetic mean	Standard deviation	N
Forest soil	WDPT (s)	1	7100	8	641 ***	1499	39
	k(–2 cm) (m s^{-1})	8.33×10^{-8}	1.96×10^{-5}	1.88×10^{-6}	4.60×10^{-6} ***	6.21×10^{-6}	10
	S_w(–2 cm) (m s$^{-1/2}$)	1.70×10^{-5}	6.58×10^{-4}	4.70×10^{-5}	1.85×10^{-4} ***	2.07×10^{-4}	11
	S_e(–2 cm) (m s$^{-1/2}$)	9.31×10^{-4}	4.52×10^{-3}	1.53×10^{-3}	2.26×10^{-3}	1.41×10^{-3}	11
	R (–)	3.57	360.2	38.6	100.5 ***	122.4	11
	K_s Equation (5) (m s^{-1})	4.80×10^{-5}	2.50×10^{-4}	1.18×10^{-4}	1.34×10^{-4} ***	6.78×10^{-5}	11
	K_s Equation (6) (m s^{-1})	2.43×10^{-5}	1.67×10^{-4}	$8.23\text{x}10^{-5}$	8.21×10^{-5} ***	4.93×10^{-5}	8
	ECS (m^2 m^{-2})	0.725	0.851	0.815	0.805 *	0.0447	6
	DPF (–)	0.0441	0.133	0.0720	0.0777 *	0.0303	6
Pure sand	WDPT (s)	1	1	1	1 ***	0	39
	k(–2 cm) (m s^{-1})	1.45×10^{-4}	7.80×10^{-4}	4.61×10^{-4}	4.78×10^{-4} ***	2.17×10^{-4}	9
	S_w(–2 cm) (m s$^{-1/2}$)	2.93×10^{-3}	1.17×10^{-2}	7.13×10^{-3}	7.60×10^{-3} ***	2.95×10^{-3}	9
	S_e(–2 cm) (m s$^{-1/2}$)	9.97×10^{-4}	3.98×10^{-3}	2.78×10^{-3}	2.68×10^{-3}	8.76×10^{-4}	9
	R (–)	0.28	1.85	0.644	0.816 ***	0.498	9
	K_s Equation (5) (m s^{-1})	3.32×10^{-4}	7.04×10^{-4}	5.31×10^{-4}	5.23×10^{-4} ***	1.37×10^{-4}	8
	K_s Equation (6) (m s^{-1})	2.50×10^{-4}	1.51×10^{-3}	2.93×10^{-4}	5.14×10^{-4} ***	4.46×10^{-4}	7
	ECS (m^2 m^{-2})	0.839	0.882	0.874	0.868 *	0.0164	5
	DPF (–)	0.0249	0.0574	0.0331	0.0364 *	0.0132	5

N is a number of replicates.
* and *** denote the properties which are significantly different between soils on significance level 0.05 and 0.001, respectively.

It should be noted that one of 8 estimates of K_s from Eq. (6) in pure sand and three of 11 estimates of K_s from Eq. (6) in forest soil were rejected because the C_1C_3 product in this equation was negative.

The mean values of both the persistence (WDPT) and index of water repellency in the pine forest soil were about 640- and 120-times higher than those of the pure sand, respectively, and they differed significantly from those of pure sand (Table 2). However, the variability in water repellency is high, which is in agreement with the findings of Lamparter et al. (2010). Almost 50% of field-moist samples taken in April–September were wettable, which is consistent with findings of García et al. (2005) who detected 57% wettable field-moist samples (N = 89), taken at depths 0–0.025 m under the *Pinus pinea* trees in southern Spain in March–November. Relative

frequency of slightly, strongly, severely, and extremely repellent field-moist samples ($N = 39$) from our site was 5, 23, 18, and 5%, respectively. Buczko et al. (2006) detected 60% wettable, 18% slightly, 2% strongly, and 10% extremely repellent field-moist samples ($N = 70$), taken at depths 0–0.1 m under 84-year old Scots pine (*Pinus sylvestris*) trees in northeast Germany in April, July, and October–December.

The mean values of water sorptivity, hydraulic conductivity, and saturated hydraulic conductivity in the forest soil were 1%, 2.4%, and 26% of those of the pure sand, respectively, and they differed significantly from those of pure sand (Table 2). The mean and median values of saturated hydraulic conductivity (1.34×10^{-4} m s^{-1} and 1.18×10^{-4} m s^{-1}) accord with those determined by Buczko et al. (2006) with a single-ring infiltrometer (with a ring diameter of 20 cm and ponded depth of about 20 cm) under Scots pine trees in northeast Germany (1.3×10^{-4} m s^{-1} and 9.06×10^{-5} m s^{-1}, respectively).

The change in soil hydrophysical parameters due to soil water repellency resulted in preferential flow in the forest soil, emerging during a simulated heavy rain following a long hot, dry period. Based on the ponded area observed during water application, we attribute the preferential flow-like shape of the wetting front to redistribution of applied water on the surface to the series of micro-catchments, which acted as runon and runoff zones. The vertical section exposed at a distance of 60 cm from the leading edge is shown in Fig. 1a. The plot of the cumulative water content changes against the cumulative cross-sectional area (black dots), ECS and DPF for the above-mentioned vertical section are presented in Fig. 1b.

The wetting front in pure sand exhibited a form typical of that for stable flow (Lichner et al. 2010). Such a shape of the wetting front can be expected in the forest soil in spring, when soil water repellency is alleviated substantially (Wessolek et al. 2008).

Conclusion

It was found that Scots pine (*Pinus sylvestris*) trees had a strong influence on hydrophysical parameters of an aeolian sandy soil during hot and dry spells. The change in soil hydrophysical parameters due to soil water repellency resulted in preferential flow in the forest soil, emerging during a simulated heavy rain following a long hot, dry period. The wetting front in pure sand exhibited a form typical of that for stable flow. Such a shape of the wetting front can be expected in vegetation covered sub-sites in spring, when soil water repellency is alleviated substantially.

Acknowledgements

The authors thank Dr. M. Šír (Institute of Hydrodynamics AS CR, Prague, Czech Republic), Dr. T. Orfánus (Institute of Hydrology SAS, Bratislava, Slovakia), Š. Aschenbrenner and Dr. M. Homolák (Technical University Zvolen, Zvolen, Slovakia) for their assistance in field measurements, and K. Schacht (Ruhr-University Bochum, Bochum, Germany) for his assistance in processing the vertical sections. This work was supported by the Scientific Grant Agency VEGA Project No. 2/0073/11 and Slovak-Polish Project SK-PL-0025-2010. This publication is the result of the project implementation ITMS 26240120004 Centre of excellence for integrated flood protection of land supported by the Research & Development Operational Programme funded by the ERDF.

References

Beatty S.M. & Smith J.E. 2013. Dynamic soil water repellency and infiltration in post-wildfire soils. Geoderma **192:** 160–172.

Buczko U., Bens O. & Hüttl R.F. 2006. Water infiltration and hydrophobicity in forest soils of a pine–beech transformation chronosequence. J. Hydrol. **331:** 383–395.

CAB International 2002. Pines of Silvicultural Importance. CABI Publishing, Wallingford.

Decagon 2007. Minidisk Infiltrometer User's Manual. Decagon Devices, Inc., Pullman.

Doerr S.H., Shakesby R.A. & Walsh R.P.D. 2000. Soil water repellency: its causes, characteristics and hydro-geomorphological significance. Earth-Sci. Rev. **51:** 33–65.

García F.J.M., Dekker L.W., Oostindie K. & Ritsema C.J. 2005. Water repellency under natural conditions in sandy soils of southern Spain. Aust. J. Soil Res. **43:** 291–296.

Hallett P.D., Baumgartl T. & Young I.M. 2001. Subcritical water repellency of aggregates from a range of soil management practices. Soil Sci. Soc. Am. J. **65:** 184–190.

Homolák M., Capuliak J., Pichler V. & Lichner Ľ. 2009. Estimating hydraulic conductivity of a sandy soil under different plant covers using minidisk infiltrometer and a dye tracer experiment. Biologia **64:** 600–604.

Kutílek M. & Krejča M. 1987. Three-parameter infiltration equation of Philip type (in Czech). Vodohosp. Čas. **35:** 52–61.

Kutílek M. & Nielsen D.R. 1994. Soil Hydrology. Catena, Cremlingen-Destedt, 370 pp.

Lamparter A., Bachmann J. & Woche S.K. 2010. Determination of small-scale spatial heterogeneity of water repellency in sandy soils. Soil Sci. Soc. Am. J. **74:** 2010–2012.

Levene H. 1960. Robust tests for equality of variances, pp. 278–292. In: Olkin, I. et al. (eds), Contributions to Probability and Statistics. Stanford University Press, Palo Alto.

Lichner L., Hallett P.D., Orfánus T., Czachor H., Rajkai K., Šír M. & Tesař M. 2010. Vegetation impact on the hydrology of an aeolian sandy soil in a continental climate. Ecohydrol. **3:** 413–420.

Lichner L., Eldridge D.J., Schacht K., Zhukova N., Holko L., Šír M. & Pecho J. 2011. Grass cover influences hydrophysical parameters and heterogeneity of water flow in a sandy soil. Pedosphere **21:** 719–729.

Lichner L., Holko L., Zhukova N., Schacht K., Rajkai K., Fodor N. & Sándor R. 2012. Plants and biological soil crust influence the hydrophysical parameters and water flow in an aeolian sandy soil. J. Hydrol. Hydromech. **60:** 309–318.

Müller K. & Deurer M. 2011. Review of the remediation strategies for soil water repellency. Agric. Ecosyst. Environ. **144:** 208–221.

Pekárová P., Svoboda A., Miklánek P., Škoda P., Halmová D. & Pekár J. 2012. Estimating flash flood peak discharge in Gidra and Parná basin: case study for the 7–8 June 2011 flood. J. Hydrol. Hydromech. **60:** 206–216.

Soil Survey Division Staff 1993. Soil survey manual. Soil Conservation Service. U.S. Department of Agriculture Handbook 18, 437 pp.

Täumer K., Stoffregen H. & Wessolek G. 2006. Seasonal dynamics of preferential flow in a water repellent soil. Vadose Zone J. **5:** 405–411.

Wessolek G., Schwärzel K., Greiffenhagen A. & Stoffregen H. 2008. Percolation characteristics of a water-repellent sandy forest soil. Eur. J. Soil Sci. **59:** 14–23.

Wine M.L., Ochsner T.E., Sutradhar A. & Pepin R. 2012. Effects of eastern redcedar encroachment on soil hydraulic properties along Oklahoma's grassland-forest ecotone. Hydrol. Process. **26:** 1720–1728.

WRB 2006. World Reference Base for Soil Resources 2006. 2nd edition. World Soil Resources Reports No. 103. FAO, Rome.

Zhang R. 1997. Determination of soil sorptivity and hydraulic conductivity from the disk infiltrometer. Soil Sci. Soc. Am. J. **61:** 1024–1030.

Received January 31, 2013
Accepted May 9, 2013